Regular Article

PHYSICAL CHEMISTRY RESEARCH
Published by the
Iranian Chemical Society
www.physchemres.org
info@physchemres.org

***Phys. Chem. Res.**, Vol. 4, No. 3, 451-467, September 2016*

Theoretical Calculations of the Effect of Finite Length on the Structural Properties of Pristine and Nitrogen-doped Carbon Nanotubes

F. Shojaie

Department of Photonic, Institute of Science and High Technology and Environmental Sciences, Graduate University of Advanced Technology, P.O. Box: 76315-117, Kerman, Iran

(Received 23 February 2016, Accepted 11 May 2016)

The effect of impurities on quantum chemical parameters of single-walled nanotubes (SWNTs) was studied using density functional theory (DFT). The density of states (DOS), Fermi energy and thermodynamic energies of (5,5) carbon nanotubes were calculated in the presence of nitrogen impurity. It was found that this nanotube remains metallic after being doped with one nitrogen atom. The partial density of states (PDOS) of spin up and spin down electrons shows that the SWNTs and nitrogen doped single-walled nanotubes (N-SWNTs) are anti-ferromagnetic. Comparing the results of SWNTs with N-SWNTs, it can be shown that there is a relationship between the energy gap and the DOS. The relationship between the thermodynamic properties and the binding energies of nanotubes is similar to the energy gap and the DOS relation.

Keywords: Density of states, Binding energy, Single-walled nanotube, Fermi energy, Anti-ferromagnetic

INTRODUCTION

SWNTs with their interesting properties have opened up several fields in nanotechnology since their discovery by Iijima [1]. The unique properties of carbon nanotubes have made them useful in different kinds of applications such as drug delivery [2,3], sensors [4,5], catalysts [6,7] and hydrogen storage [8,9]. Also, properties of carbon nanotubes are among the most interesting subjects and many studies have been focussed on their structural, electronic and mechanical properties [10-12]. The electrical properties of nanotubes may be changed by their length [13]. Rochefort *et al.* showed that the band-gap of armchair carbon nanotubes decreases with increasing tube length. Although this band-gap decrease is not monotonic, it describes a well-defined oscillation in short tubes [14]. Petrushenko *et al.* studied the electronic and structural properties of armchair (5,5) SWNTs and investigated ionization potential and electron affinity (vertical and adiabatic) for a series of SWNTs as a function of the tube length by means of the DFT [15]. In addition, study of the electronic properties of doped SWNTs is one of the most interesting subjects, especially as gas detecting sensors [16,17] and biosensors [18]. In this paper, structural properties and reactivity of armchair (5,5) SWNTs in the absence and presence of nitrogen impurity (N-SWNTs) are investigated by DFT. The changes in electronic and structural properties of SWNTs and N-SWNTs are studied in gaseous and aqueous phase.

*Corresponding author. E-mail: f.shojaie@kgut.ac.ir

RESULTS AND DISCUSSION

Computational Methods

The $C_{20n}H_{20}$ and $C_{20n-1}NH_{20}$ (n = 4, 6, 8) models were used for pristine and nitrogen-doped carbon nanotubes, respectively. All calculations of CNT properties were performed by DMol3 code [19,20] which is based on DFT. The Double Numerical basis set with Polarization functions

(DNP) was also used for calculations of CNT properties. This basis set is comparable with the Gaussian 6-31G (d,p) set. The main calculations presented in this work are based on the Generalized Gradient Approximation corrections (GGA) methods developed by Perdew and Wang (PW91) and Becke-Lee-Yang-Parr (BLYP) [21-24]. All electrons were taken into account in order to depict core states. Total energy convergence criteria for Self-Consistent Field (SCF) was set at 10^{-6} eV. A smearing of 0.005 Hartree was considered to improve computational performance in terms of fast SCF convergence. Full geometrical optimization was performed by examining species in gaseous and aqueous phase. The effect of water on SWNTs and N-SWNTs was estimated by the Conductor-like Screening Model (COSMO) [25]. The dielectric constant of water was set at 78.54 in the COSMO model. All structures were considered to be minima based on the absence of imaginary frequencies which provides a true minimum on the potential surface. The effects of quantum chemical parameters on SWNTs and N-SWNTs were studied using six stable configuration models, as presented in Fig. 1. These six models are $C_{80}H_{20}$, $C_{120}H_{20}$, $C_{160}H_{20}$, $C_{79}NH_{20}$, $C_{119}NH_{20}$, $C_{159}NH_{20}$, $C_{80}H_{20}$, $C_{120}H_{20}$ and $C_{160}H_{20}$. $C_{80}H_{20}$, $C_{120}H_{20}$, $C_{160}H_{20}$ models are C (5,5) pristine carbon nanotubes and $C_{79}NH_{20}$, $C_{119}NH_{20}$ and $C_{159}NH_{20}$ models are nitrogen-doped carbon nanotubes.

Quantum Chemical Parameters

The quantum chemical parameters give information on the chemical reactivity of molecules. The gap between the HOMO and LUMO energy levels is an important function of reactivity of a molecule. Figure 2 shows the energy gaps, calculated by BLYP and PW91 methods, for the six models in gaseous and aqueous phase. The trends of the quantum chemical parameters are almost similar in both phases. $C_{120}H_{20}$ pristine carbon nanotube has a low energy gap in both phases, in agreement with the energy gap given in reference [13]. These low energy gaps show that an electron transfer from the $C_{120}H_{20}$ HOMO to its LUMO occurs more easily than that from HOMOs of $C_{80}H_{20}$ and $C_{160}H_{20}$ to their LOMOs in both phases. The energy gaps of $C_{79}NH_{20}$ and $C_{159}NH_{20}$ are lower than those in pristine carbon nanotube counterparts *i.e.* $C_{80}H_{20}$ and $C_{160}H_{20}$. Figure 2 shows that $C_{120}H_{20}$ has a lower energy gap than $C_{80}H_{20}$ and $C_{160}H_{20}$ in both phases. A smaller energy gap leads to a larger electric

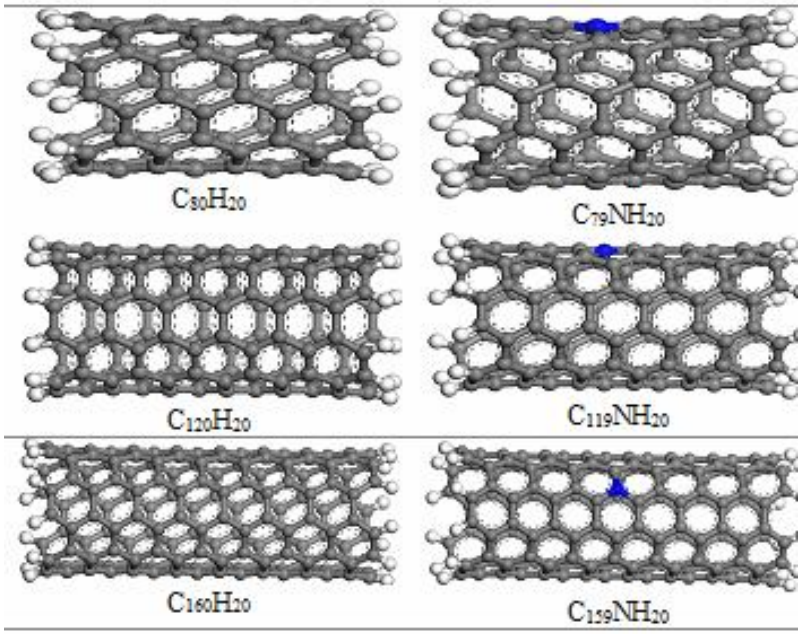

Fig. 1. The optimized structures of pristine and nitrogen-doped carbon nanotubes.

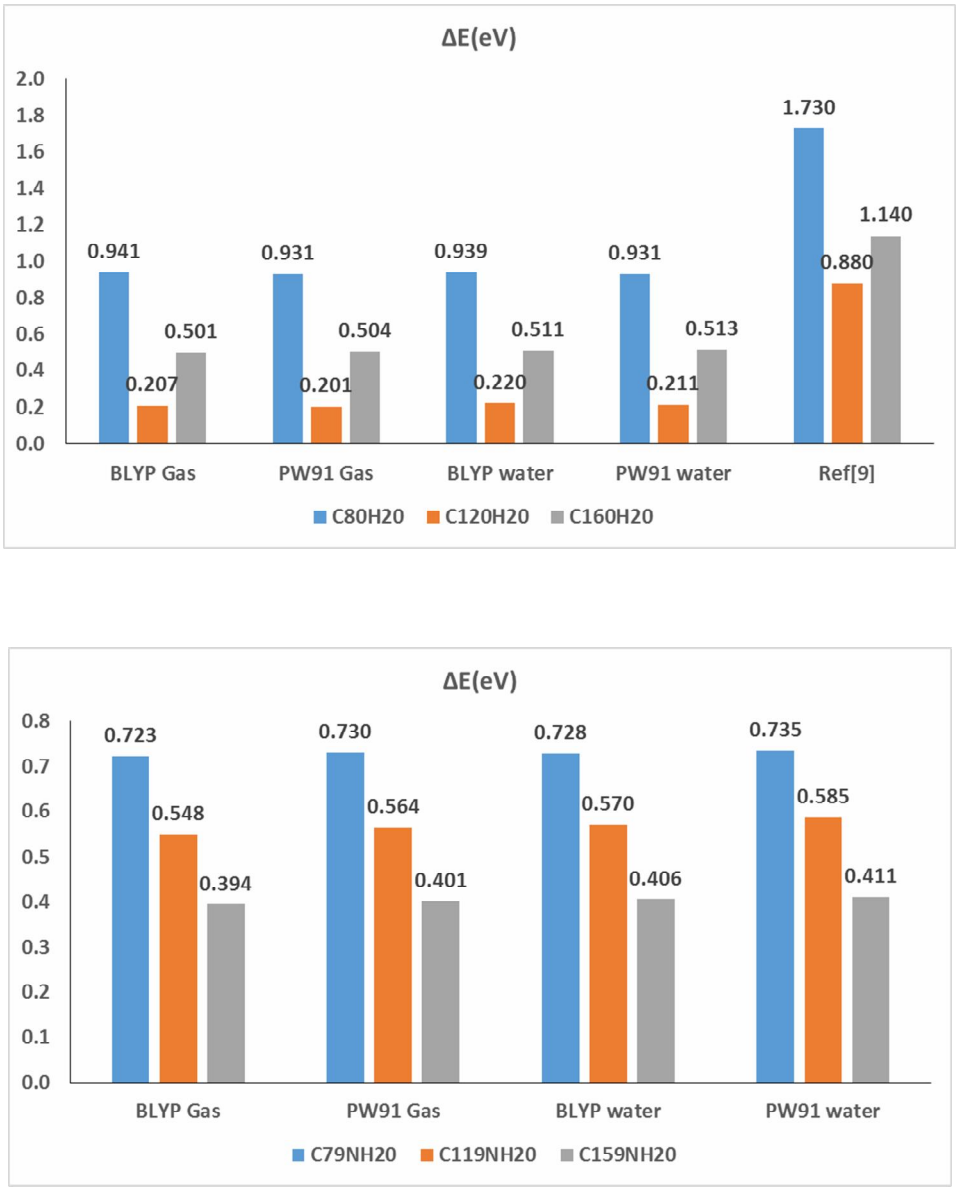

Fig. 2. Diagram of energy gap for SWNT and N-SWNT.

conductivity at a given temperature. Therefore, $C_{120}H_{20}$ has a higher electric conductivity than $C_{80}H_{20}$ and $C_{160}H_{20}$. Electric conductivity of $C_{120}H_{20}$ decreases with nitrogen doping, in contrast to the decreases in electric conductivities of $C_{80}H_{20}$ and $C_{160}H_{20}$ with nitrogen doping.

Ionization Potential (IP) is a basic descriptor of the chemical reactivity of atoms and molecules. A high IP shows a towering stability. Tables 1 and 2 show that ionization energies of $C_{120}H_{20}$, calculated by orbital and energy modes of BLYP/PW91 method are lower than those of $C_{80}H_{20}$ and $C_{160}H_{20}$ in both phases whereas electron affinities of $C_{120}H_{20}$ are higher than those of $C_{80}H_{20}$ and $C_{160}H_{20}$. $C_{159}NH_{20}$ has the lowest ionization energy, except values obtained by the orbital mode, and the highest electron affinity among nitrogen-doped carbon nanotubes in both phases.

Table 1. The Ionization Potential for Pure and N-doped Carbon Nanotubes

Compounds	IP (eV)									
	IP = [E(+1) - E(0)] (Energetic)					IP = $-E_{HOMO}$ (Orbital)				
	Gas			Liquid		Gas			Liquid	
	PW91	BLYP	Others	PW91	BLYP	PW91	BLYP	Others	PW91	BLYP
$C_{80}H_{20}$	5.577	5.311	5.48[a]	4.586	4.295	4.248	3.993	4.480[a]	4.443	4.161
			5.28[b]					4.28[b]		
$C_{120}H_{20}$	5.160	4.887	5.00[a]	4.289	3.990	3.990	3.729	4.159[a]	4.156	3.868
			4.83[b]					3.96[b]		
$C_{160}H_{20}$	5.250	4.969	5.10[a]	4.462	4.153	4.197	3.927	4.350[a]	4.338	4.039
			4.90[b]					4.14[b]		
$C_{99}NH_{20}$	5.081	4.820	-	4.065	3.778	4.285	4.028	-	4.463	4.180
$C_{119}NH_{20}$	5.059	4.785	-	4.165	3.864	3.920	3.658	-	4.063	3.772
$C_{159}NH_{20}$	4.669	4.385	-	3.854	3.544	4.237	3.967	-	4.360	4.062

[a]Ref. [11]. [b]Ref. [9].

Table 2. The Electron Affinity for SWNT and N-SWNT

Compounds	EA(eV)									
	EA = [E(0) - E(-1)] (Energetic)					EA = $-E_{LUMO}$ (Orbital)				
	Gas			Liquid		Gas			Liquid	
	PW91	BLYP	Others	PW91	BLYP	PW91	BLYP	Others	PW91	BLYP
$C_{80}H_{20}$	2.100	1.842	1.55[a]	3.392	3.101	3.309	3.052	2.55[a]	3.512	3.230
$C_{120}H_{20}$	2.768	2.497	2.21[a]	3.871	3.566	3.789	3.523	3.08[a]	3.945	3.648
$C_{160}H_{20}$	2.804	2.532	2.23[a]	3.780	3.473	3.692	3.426	3.00[a]	3.825	3.528
$C_{99}NH_{20}$	2.194	1.947	-	3.464	3.183	3.554	3.305	-	3.728	3.452
$C_{119}NH_{20}$	2.672	2.410	-	3.763	3.467	3.356	3.110	-	3.478	3.202
$C_{159}NH_{20}$	3.181	2.920	-	4.139	3.843	3.836	3.573	-	3.949	3.656

[a]Ref. [9].

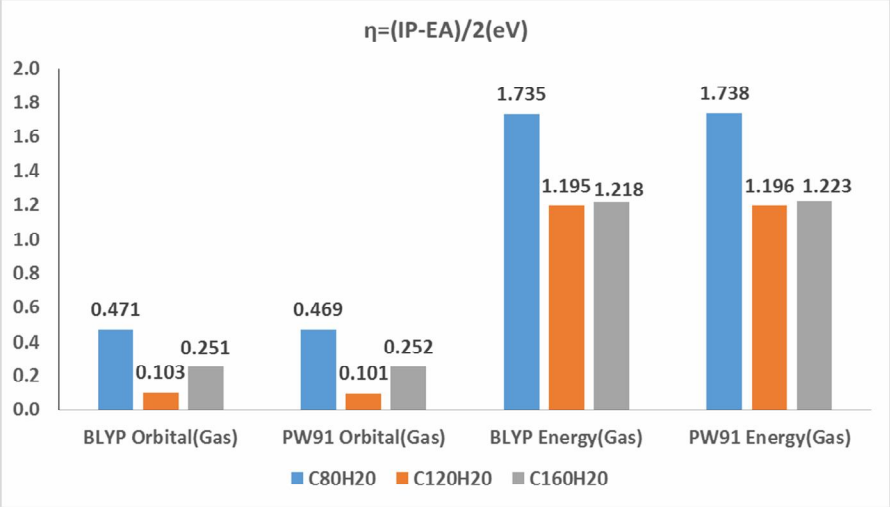

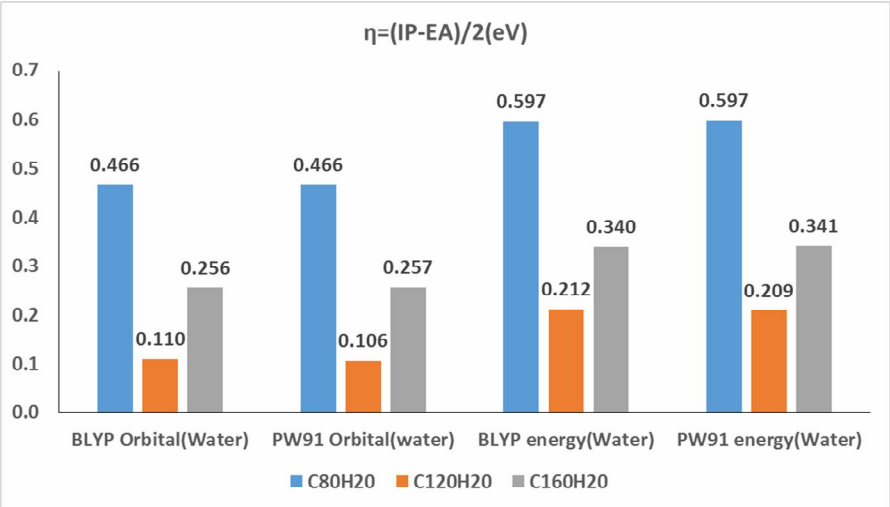

Fig. 3. Diagram of global hardness for pure and N-doped carbon nanotubes.

The absolute hardness and softness are important properties for measuring a molecular stability and reactivity. Based on absolute hardness and softness parameters, $C_{120}H_{20}$ is a soft molecule with higher reactivity than $C_{80}H_{20}$ and $C_{160}H_{20}$ in both phases. The $C_{159}NH_{20}$ has the highest reactivity among nitrogen-doped carbon nanotubes (See Fig. 3).

The ability of a molecule to accept electrons may be described by its electrophilicity index. It is a measure of stabilization energy after the system accepts the additional amount of electron charge from its environment. Table 3 shows that the electrophilicities of $C_{160}H_{20}$ and $C_{159}NH_{20}$, calculated by orbital and energy modes of BLYP/PW91 method, are higher than those of other models. Therefore, $C_{160}H_{20}$ and $C_{159}NH_{20}$ are stronger electrophile than the other models.

The polarity of a molecule describes its dipole moment. As reported in Table 4, $C_{119}NH_{20}$ has the highest dipole moment, μ, in both phases. μ values of nitrogen-doped carbon nanotubes are higher in aqueous phase than those in gaseous phase. This illustrates the fact that polarization

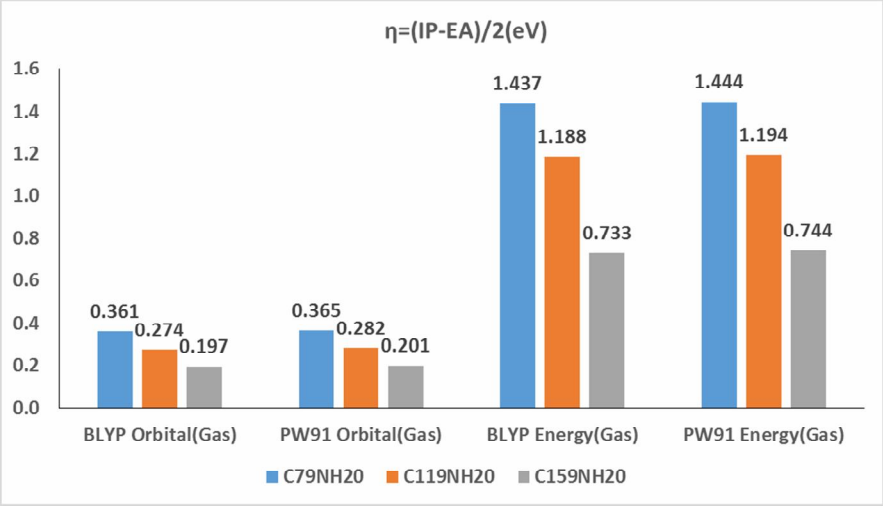

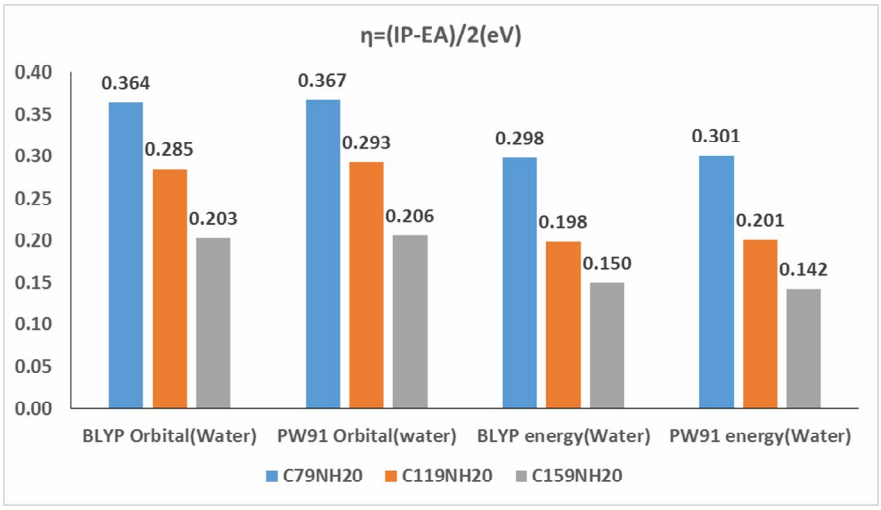

Fig. 3. Continued.

effect of the solvent on nitrogen-doped carbon nanotubes is stronger than that on the pristine nanotube molecules.

The binding energies of all carbon nanotubes are negative in both phases and slightly lower in the gaseous phase. This means that a nanotube is more stable in its aqueous phase. The binding energies of all nitrogen-doped carbon nanotube are higher than those in pristine forms in both phases.

Therefore, a pristine carbon nanotube is more stable than nitrogen-doped carbon nanotube. Figure 5 shows that $C_{160}H_{20}$ and $C_{159}NH_{20}$ have the highest solubility in water among pristine and nitrogen-doped carbon nanotubes. The dielectric solvation energy of $C_{79}NH_{20}$ is higher than that of $C_{80}H_{20}$ and this is especially more obvious in the case of the solvation energies calculated by BLYP method. However, the dielectric solvation energies of the other two nitrogen-doped carbon nanotubes are lower than those in their pristine counterparts.

DOS

PDOS, with consideration of the electronic spin polarization, may be employed to find a material

Table 3. The Electronegativity for Pure and N-doped Carbon Nanotubes

Compounds	Electronegativity (χ) (eV) $\chi = (IP + EA)/2$							
	Energetic				Orbital			
	Gas		Liquid		Gas		Liquid	
	PW91	BLYP	PW91	BLYP	PW91	BLYP	PW91	BLYP
$C_{80}H_{20}$	3.838	3.576	3.989	3.698	3.778	3.523	3.978	3.695
$C_{120}H_{20}$	3.964	3.692	4.080	3.778	3.890	3.626	4.051	3.758
$C_{160}H_{20}$	4.027	3.750	4.121	3.813	3.945	3.676	4.081	3.784
$C_{99}NH_{20}$	3.638	3.383	3.765	3.481	3.920	3.666	4.096	3.816
$C_{119}NH_{20}$	3.865	3.598	3.964	3.665	3.638	3.384	3.770	3.487
$C_{159}NH_{20}$	3.925	3.653	3.996	3.693	4.037	3.770	4.154	3.859

Table 4. The Dipole Moment for SWNT and N-SWNT

Compounds	Gas		Liquid	
	PW91	BLYP	PW91	BLYP
$C_{80}H_{20}$	0.003	0.003	0.004	0.004
$C_{120}H_{20}$	0.003	0.004	0.003	0.003
$C_{160}H_{20}$	0.005	0.005	0.003	0.005
$C_{99}NH_{20}$	1.972	1.972	4.660	4.520
$C_{119}NH_{20}$	2.309	2.229	5.487	5.362
$C_{159}NH_{20}$	1.977	1.901	4.865	4.736

composition which may then be used to determine its band structure. The DOS and PDOS for pure and doped (5,5) armchair carbon nanotubes are given in Figs. 6, 7 and 8. The energy eigenvalues were smeared with gaussians width, σ, of 0.19 eV and PDOS, with consideration of the electronic spin polarization, were employed for SWNTs. Figures 6, 7 and 8 show that the DOS between the valence band and the conduction band is not zero and thus there are no impediments for the electrons to flow between two bands. The energy gaps of the systems are in the ranges 0.941-0.201 eV and 0.730-0.394 eV for pristine and nitrogen-doped carbon nanotubes, respectively. Our results show that these nanotubes have metallic behaviour. Figures 6a, 7a, 8a, 6b, 7b and 8b show that the differences between the PDOS of the gaseous nanotubes and those of their aqueous counterparts are very small and the trends of the

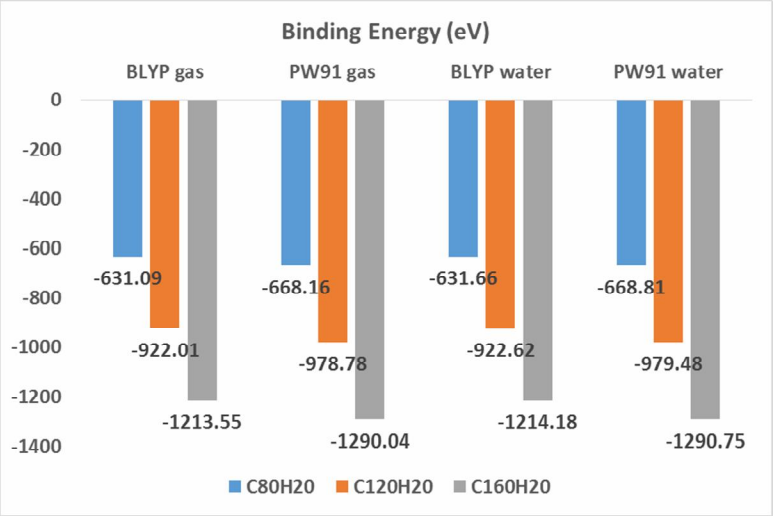

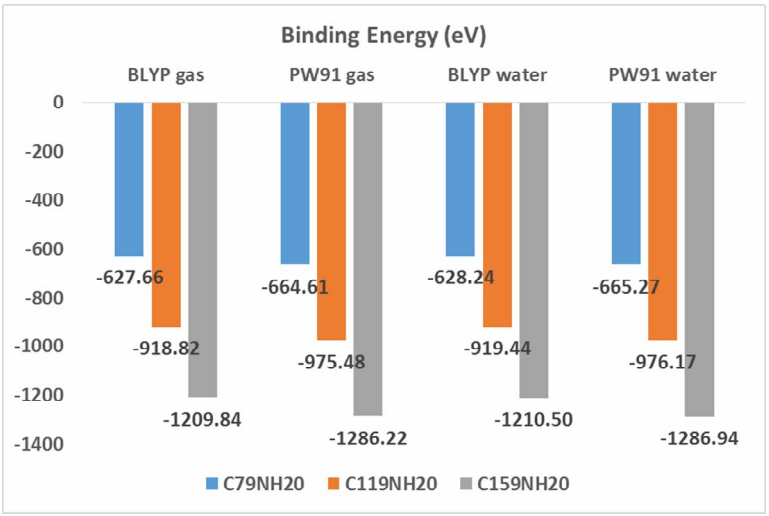

Fig. 4. Diagram of binding energy for SWNT and N-SWNT.

PDOS in the two phases are almost similar. The PDOS trend is similar to the trend of the energy gap. The p orbitals contribute most to the DOS. Figures 6c and 8c show that the DOSs of nitrogen-doped $C_{80}H_{20}$ and $C_{160}H_{20}$ vary more significantly in the valence band than they do in the conduction band. This implies that the energy gaps of $C_{80}H_{20}$ and $C_{160}H_{20}$ will decrease after being doped with nitrogen. However, in the case of $C_{120}H_{20}$, the energy gap will increase after nitrogen doping and there is not a significant DOS variation in the valence a nd conduction band (Fig. 7c). Therefore, there is a relationship between the energy gap and the DOS. The trend of energy gap is similar to that for the DOS. BLYP/PW91 calculations indicate that the valance and conduction bands of all the carbon nanotubes are mostly formed by p, s and a small amount of d states in both phases. The d orbitals of all models are not localized in the conduction bands.

Figure 9 shows the PDOS of spin up and spin down electrons in pure and nitrogen-doped carbon nanotubes. As shown in Fig. 9, the DOSs of spin up and spin down

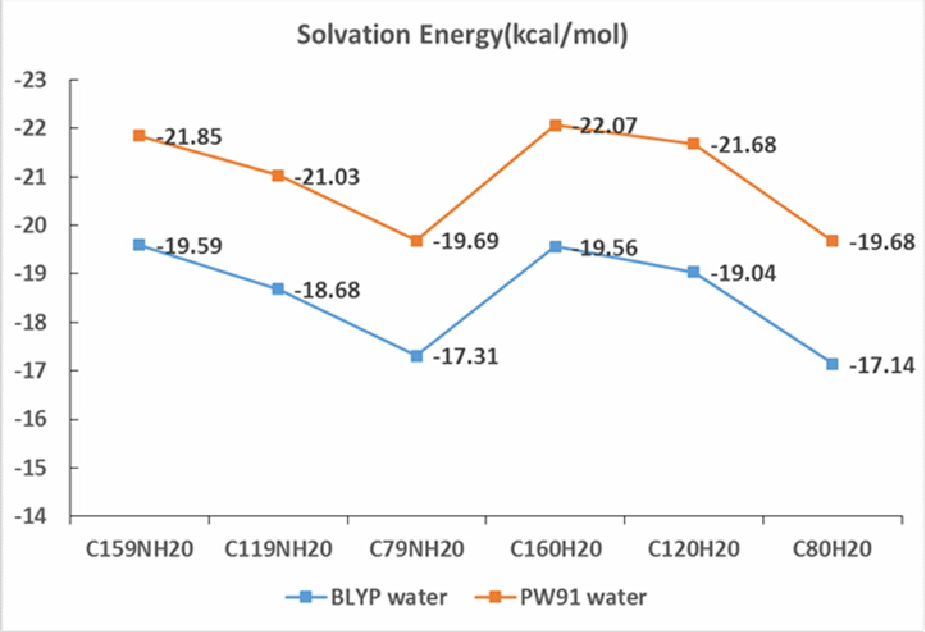

Fig. 5. Diagram of solvation energy for SWNT and N-SWNT.

electrons are equal for all values of electron energy. This means that the SWNTs and N-SWNTs are anti-ferromagnetic.

Fermi Energy

The Fermi energy, E_f, of the SWNTs and N-SWNTs is determined using the following equation: $E_f = \mu$ where μ is chemical potential. The Fermi energies of the SWNTs and N-SWNTs were calculated by the orbital and energy modes of BLYP/PW91 method. The BLYP/PW91 results show that the Fermi energy is located between HOMO and LUMO energies. However, Fig.10 shows that the Fermi energy of pristine carbon nanotubes, calculated by energy mode of BLYP/PW91 method, is closer to HOMO energy. Fermi energies of $C_{79}NH_{20}$ and $C_{159}NH_{20}$, calculated by the energy mode of BLYP/PW91 method, are closer to their LUMO energies whereas the Fermi energy of $C_{119}NH_{20}$ is closer to its HOMO energy. The difference between $C_{120}H_{20}$ Fermi energy and its HOMO energy is the lowest among the six models. $C_{120}H_{20}$ Fermi and HOMO energies are 0.026 eV and 0.037 eV. The difference between $C_{79}NH_{20}$ Fermi energy and its LUMO energy is the lowest among all the nanotubes. The $C_{79}NH_{20}$ Fermi and LUMO energies are 0.084 eV and 0.078 eV. DMol3 method uses DOS data to calculate Femi energy directly. Figure 10 shows that Fermi energies of pristine carbon nanotubes that were directly calculated by DMol3 method are the same as HOMO energies. PW91 and BLYP calculations indicate that $C_{79}NH_{20}$ and $C_{159}NH_{20}$ Fermi energies are the same as their LUMO energies and $C_{119}NH_{20}$ Fermi energy is closer to its HOMO energy. The PW91 and BLYP results are closer to the data calculated by the energy mode of BLYP/PW91 method. Therefore, pristine carbon nanotubes have metallic behaviour.

Thermodynamic Properties

Thermodynamic properties are used to describe the effects of temperature on structural stabilities. BLYP/PW91 method was used to calculate entropy (S), heat capacity (Cp), enthalpy (H) and Gibbs free energy (G) of SWNTs and N-SWNTs at different temperatures in gaseous and aqueous phase. It can be seen from Fig. 11 that the values of the G energy will gradually decrease with the elevated temperature, whereas S, Cp and H will gradually increase with rising temperature in both phases. Figure 12 may be used to compare thermodynamic properties of SWNTs with N-SWNTs at 298.15 K. Figure 12 shows that increasing tube length of carbon nanotubes will cause to increase the

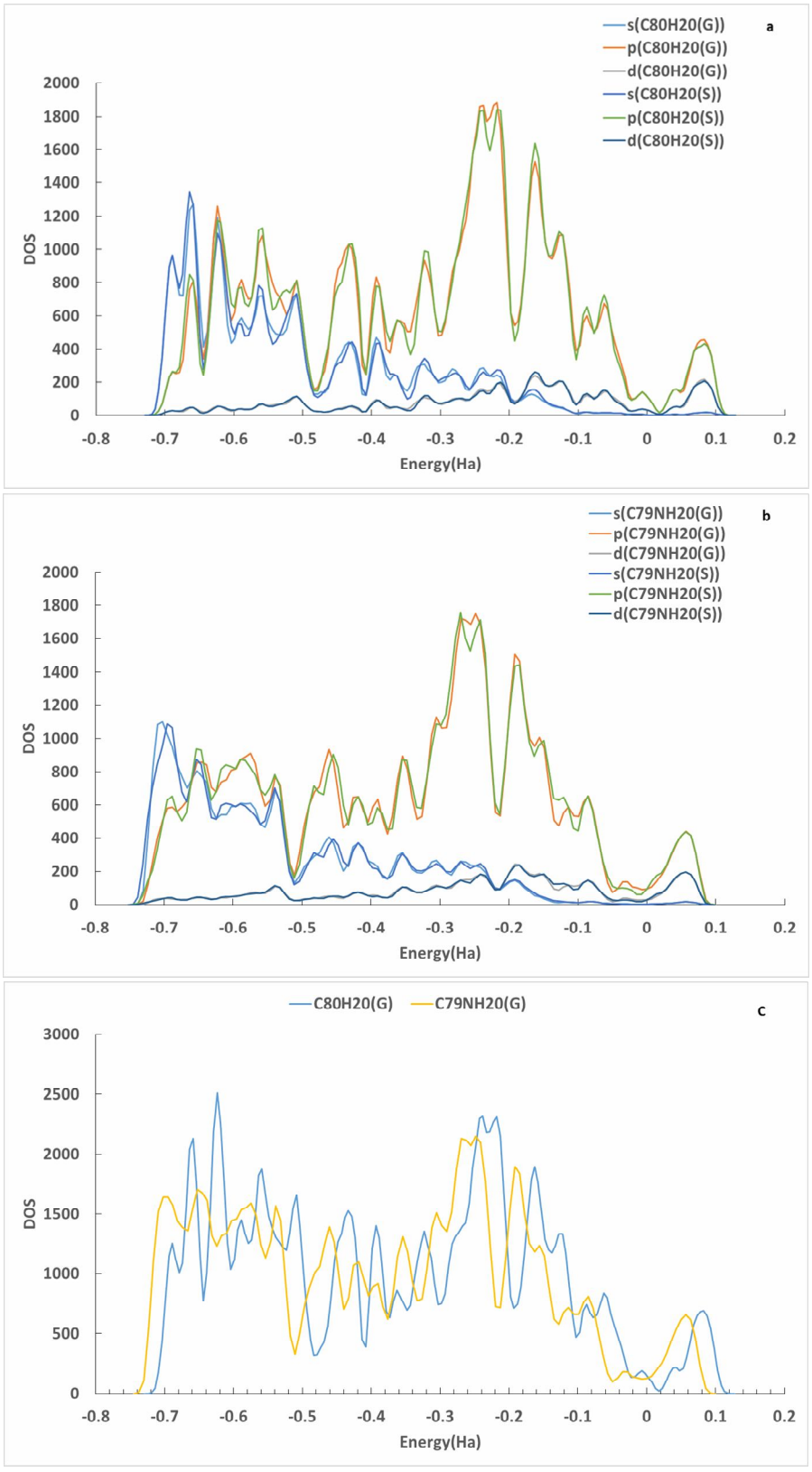

Fig. 6. The Density of states (DOS) and partial density of states (PDOS) for $C_{80}H_{20}$ and $C_{79}NH_{20}$.

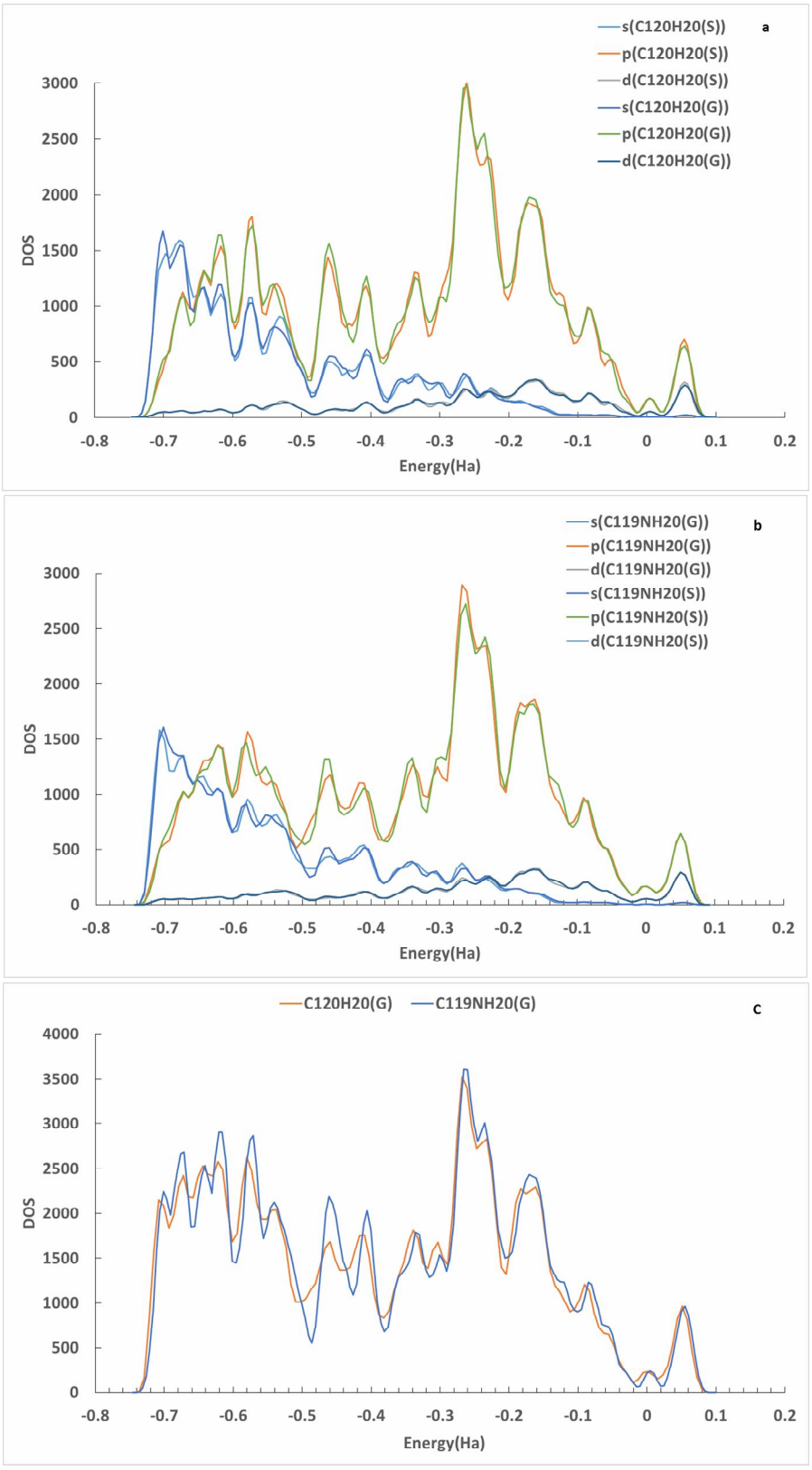

Fig. 7. The Density of states (DOS) and partial density of states (PDOS) for $C_{120}H_{20}$ and $C_{119}NH_{20}$.

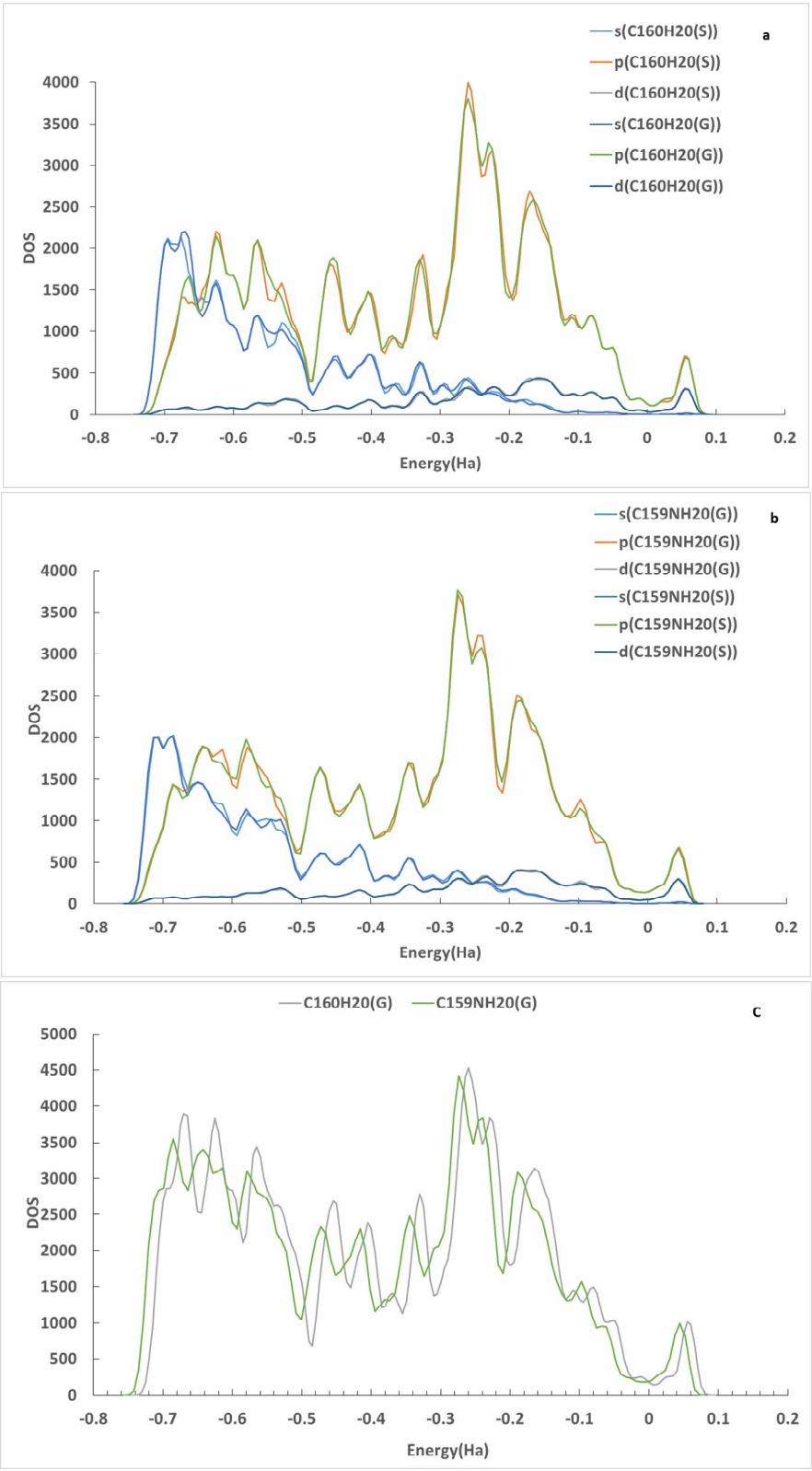

Fig. 8. The Density of states (DOS) and partial density of states (PDOS) for $C_{160}H_{20}$ and $C_{159}NH_{20}$.

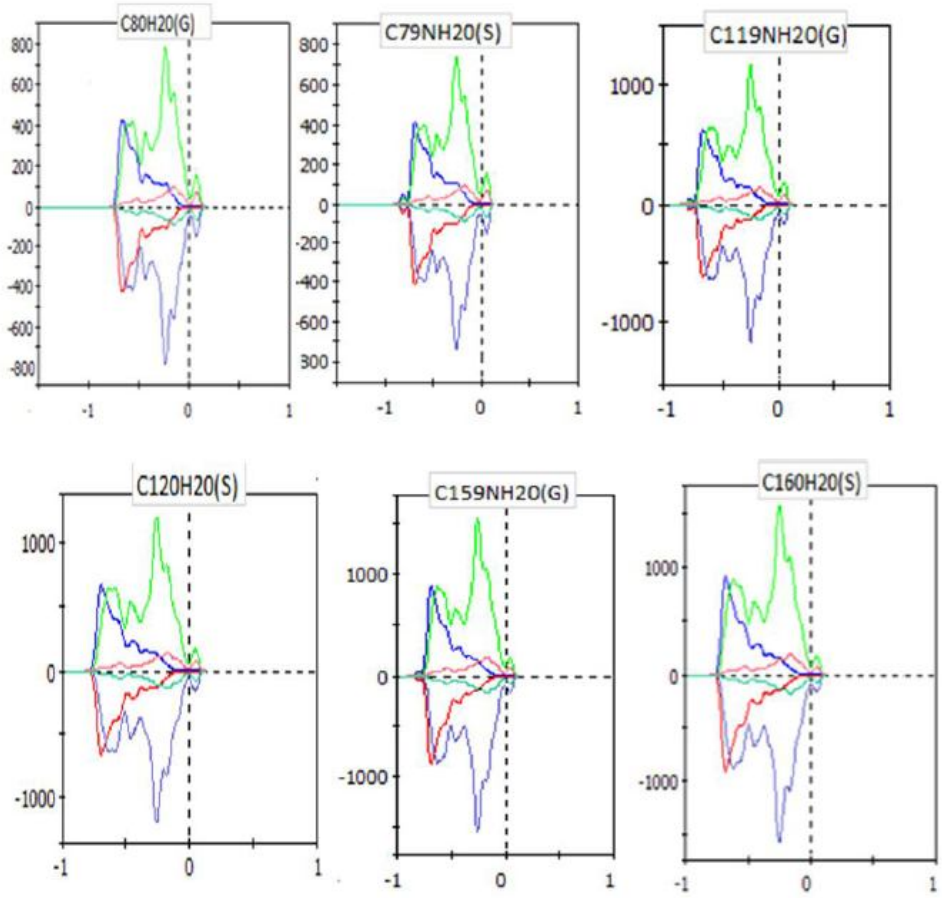

Fig. 9. The partial DOS of spin up and spin down electrons in pure and nitrogen-doped carbon nanotubes.

values of thermodynamic properties. If a compound has a small G energy, then it will have a better thermal stability [24]. The thermal stability of nitrogen-doped carbon nanotubes is better than that of pure carbon nanotubes in both phases. The thermal stability of nanotubes is better in their gaseous phase compared to that in aqueous phase. The thermodynamic energies of nanotubes have a similar trend to their binding energies.

CONCLUSIONS

The pristine carbon nanotubes, $C_{80}H_{20}$, $C_{120}H_{20}$ and $C_{160}H_{20}$, are metallic and their Fermi energies, calculated by energy mode of BLYP/PW91 method, are closer to their HOMO energies. DMol3 method uses DOS data to calculate Femi energy directly. In contrast, the Fermi energies, directly calculated by DMol3 method, are the same as HOMO energies. The $C_{120}H_{20}$ has a low energy gap and high electric conductivity in comparison to $C_{80}H_{20}$ and $C_{160}H_{20}$. The differences between the PDOSs, DOSs and the energy gaps of carbon nanotubes in gaseous form and same parameters in aqueous form are very small.

The effects of doping $C_{120}H_{20}$ with a nitrogen atom are: (a) an increase in its energy gap, (b) no clear change in the shape of the DOS, and (c) closer Fermi energy to HOMO energy. In contrast, the effects of doping $C_{80}H_{20}$ and $C_{160}H_{20}$ with nitrogen atoms are: (a) decrease in energy gap, (b) increase in electric conductivity, (c) significant change of the DOS in the valence band compared to that in the conduction band, (d) getting close the level of Fermi energies, calculated by energy mode of BLYP/PW91 method, to LUMO energies, and (e) Staying Fermi energies,

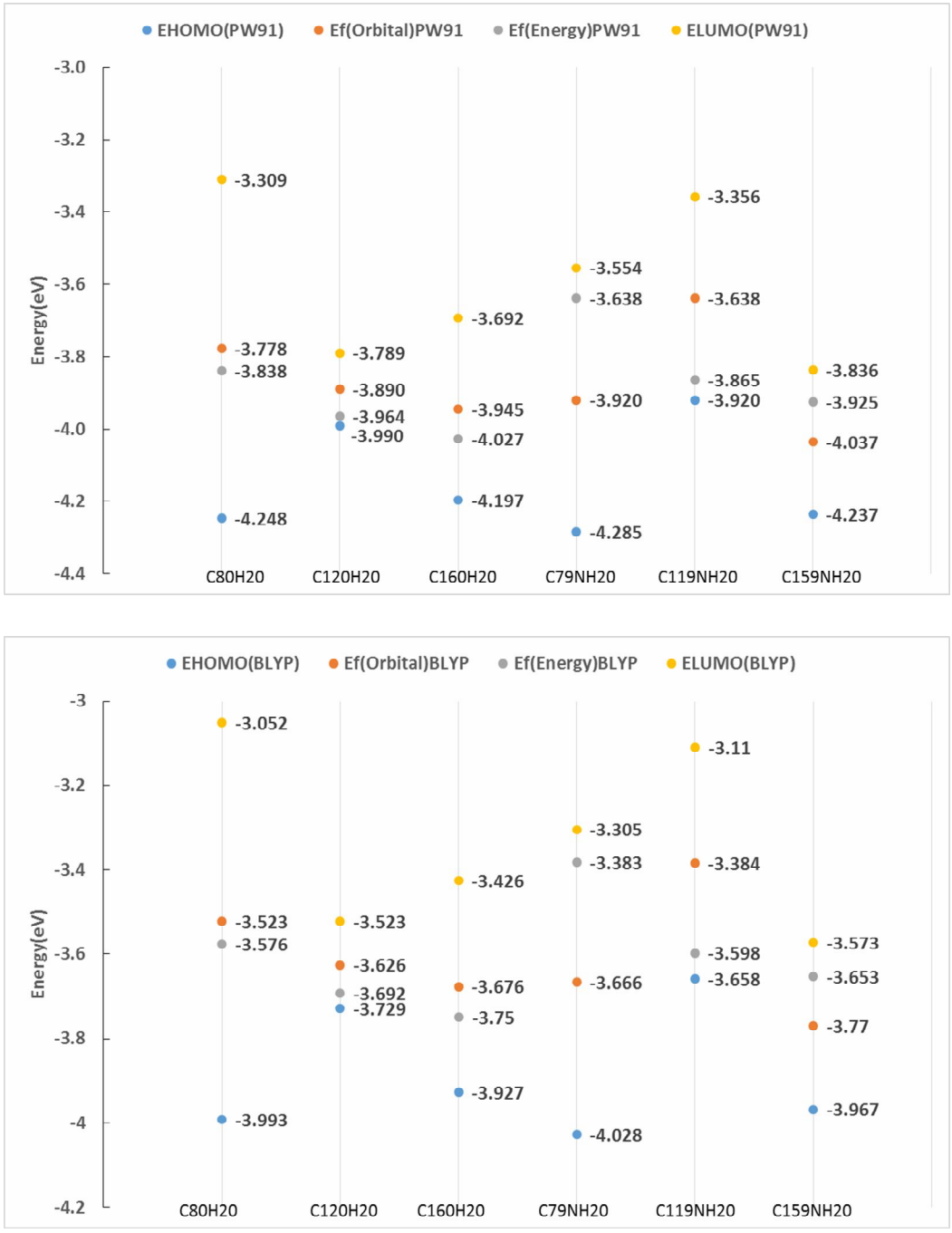

Fig. 10. Diagram of the Fermi, HOMO and LUMO energies for SWNT and N-SWNT.

directly calculated by DMol3, on LUMO energies. The data trends in gaseous phase are similar to aqueous phase.

(5,5) nanotube remains metallic after being doped with a nitrogen atom. The DOSs of spin up and spin down electrons are equal for all values of electron energy. The SWNTs and N-SWNTs are anti-ferromagnetic.

ACKNOWLEDGEMENTS

This work was supported by Graduate University of

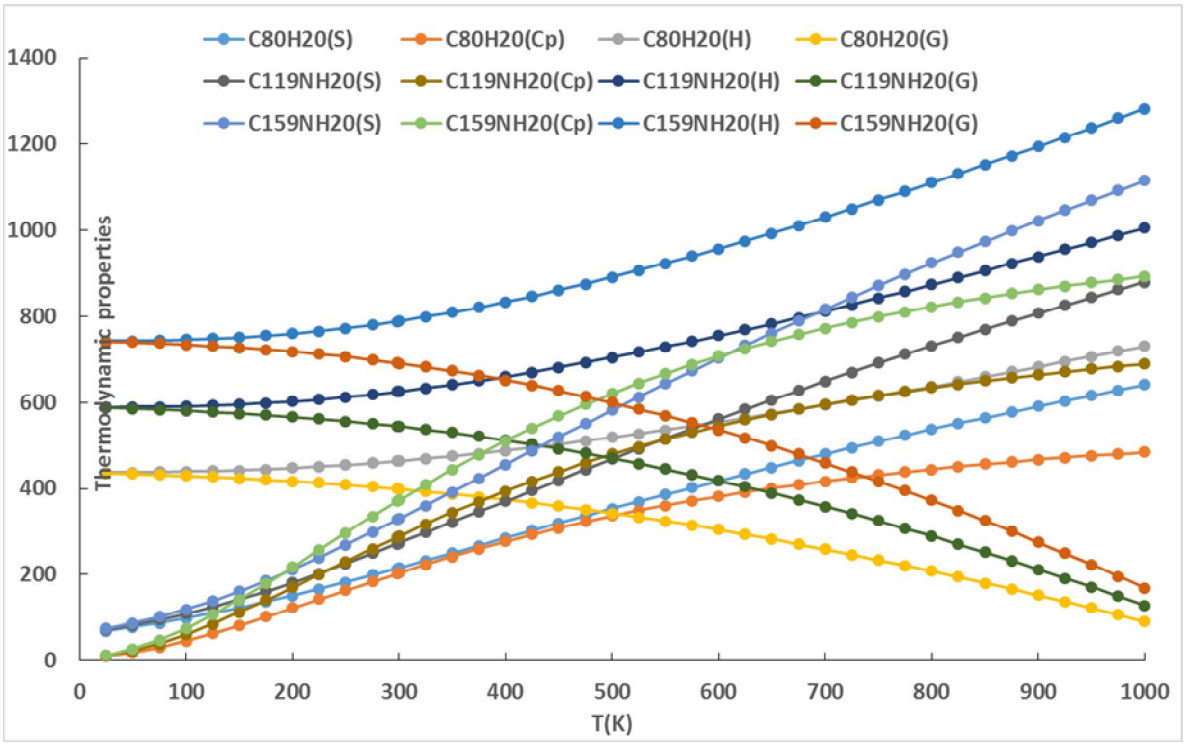

Fig. 11. Thermodynamic properties of SWNT and N-SWNT at different temperatures.

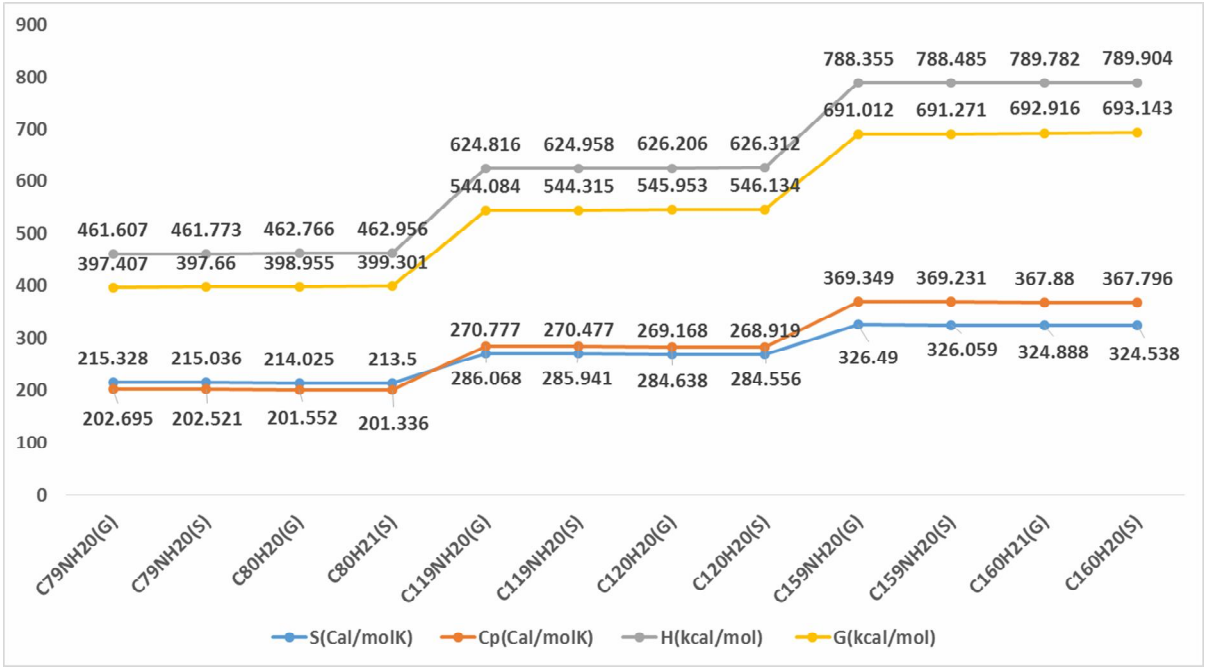

Fig. 12. Thermodynamic properties of SWNT and N-SWNT at 298.15K.

Advanced Technology and Research Center for Science, High Technology & Environmental Science, Kerman. This article was peer reviewed by Nasser Mirzai Baghini, Imperial College Reactor Centre, Silwood Park, Ascot, Berkshire, United Kingdom.

REFERENCES

[1] Iijima, S., Helical microtubules of graphitic carbon. *Nature*, **1991**, *354*, 56-58, DOI: 10.1038/354056a0.

[2] Bianco, A.; Kostarelos, K.; Prato, M., Applications of carbon nanotubes in drug delivery. *Curr. Opin. Chem. Boil.*, **2005,** *9*, 674-679, DOI: 10.1016/ j.cbpa.2005.10.005.

[3] Kostarelos, K., Rational design and engineering of delivery systems for therapeutics: biomedical exercises in colloid and surface science. *Adv .Colloid .Interface. Sic.*, **2003**, *106*, 147-168, DOI: 10.1016/ S0001-8686(03)00109-X.

[4] Kong, J.; Franklin, N. R.; Zhou, C.; Chapline, M. G.; Peng, S.; Cho, K.; Dai, H., Nanotube molecular wires as chemical sensors. *Science*, **2000**, *287*, 622-625, DOI: 10.1126/science.287.5453.622.

[5] Ghosh, S.; Sood, A.; Kumar, N., Carbon nanotube flow sensors. *Science*, **2003**, *299*, 1042-1044, DOI: 10.1126/ science.1079080.

[6] Kong, H.; Zhou, M.; Lin, G. -D.; Zhang, H. -B., Pt catalyst supported on multi-walled carbon nanotubes for hydrogenation-dearomatization of toluene and tetralin. *Catal. Lett.*, **2010**, *135*, 83-90, DOI: 10.1007/ s10562-010-0272-9.

[7] Jourdain, V.; Bichara, C., Current understanding of the growth of carbon nanotubes in catalytic chemical vapour deposition. *Carbon*, **2013**, *58*, 2-39, DOI: 10.1016/j.carbon.2013.02.046.

[8] Jones, A. D. K.; Bekkedahl, T., Storage of hydrogen in single-walled carbon nanotubes. *Nature*, **1997**, *386*, 377-379, DOI: 10.1038/386377a0.

[9] Cheng, H. -M.; Yang, Q. -H.; Liu, C., Hydrogen storage in carbon nanotubes. *Carbon*, **2001**, *39*, 1447-1454, DOI: 10.1016/S0008-6223(00)00306-7.

[10] Petrushenko, I. K.; Ivanov, N. A., DFT study of the elastic properties of pristine and moderately fluorinated single-walled carbon nanotubes. *Fuller. Nanotub. Car. N*, **2014**, *22*, 781-788, DOI: 10.1080/ 1536383X.2012.731585.

[11] Ruoff, R. S.; Qian, D.; Liu, W. K., Mechanical properties of carbon nanotubes: theoretical predictions and experimental measurements. *Comptes Rendus Physique*, **2003**, *4*, 993-1008, DOI: 10.1016/ j.crhy.2003.08.001.

[12] Yakobson, B. I.; Avouris, P., *Mechanical Properties of Carbon Nanotubes. In Carbon Nanotubes*, Springer: **2001**, p. 287-327.

[13] Zhou, Z.; Steigerwald, M.; Hybertsen, M.; Brus, L.; Friesner, R. A., Electronic structure of tubular aromatic molecules derived from the metallic (5,5) armchair single wall carbon nanotube. *J. Am. Chem. Soc.*, **2004**, *126*, 3597-3607, DOI: 10.1021/ja039294p.

[14] Rochefort, A.; Salahub, D. R.; Avouris, P., Effects of finite length on the electronic structure of carbon nanotubes. *J. Phys. Chem. B*, **1999**, *103*, 641-646, DOI: 10.1021/jp983725m.

[15] Petrushenko, I. K.; Ivanov, N. A., Onization potentials and structural properties of finite-length single-walled carbon nanotubes: DFT study. *Physica E Low Dimens. Syst. Nanostruct.*, **2013**, *54*, 262-266, DOI: 10.1016/ j.physe.2013.07.004.

[16] Mackie, I. D.; DiLabio, G. A., CO_2 adsorption by nitrogen-doped carbon nanotubes predicted by density-functional theory with dispersion-correcting potentials. *Phys. Chem. Chem. Phys.*, **2011**, *13*, 2780-2787, DOI: 10.1039/C0CP01537G.

[17] Zhang, X.; Gong, X., Theoretical investigation of rare gas adsorption on and inside B-doped carbon nanotubes by DFT, QTAIM and NBO. *RSC Advances*, **2015**, *5*, 65604-65612, DOI: 10.1039/ C5RA10657E.

[18] Xu, X.; Jiang, S.; Hu, Z.; Liu, S., Nitrogen-doped carbon nanotubes: high electrocatalytic activity toward the oxidation of hydrogen peroxide and its application for biosensing. *ACS Nano*, **2010**, *4*, 4292-4298, DOI: 10.1021/nn1010057.

[19] Delley, B., An all-electron numerical method for solving the local density functional for polyatomic molecules. *J. Chem. Phys.*, **1990**, *92*, 508-517, DOI: 10.1063/1.458452.

[20] Delley, B., Fast calculation of electrostatics in crystals

and large molecules. *J. Phys. Chem.*, **1996**, *100*, 6107-6110, DOI: 10.1021/jp952713n.

[21] Becke, A. D., A multicenter numerical integration scheme for polyatomic molecules. *J. Chem. Phys.*, **1988**, *88*, 2547-2553, DOI: 10.1063/1.454033.

[22] Becke, A. D., Density-functional thermochemistry. III. The role of exact exchange. *J. chem. Phys.*, **1993**, *98*, 5648-565, DOI: 10.1063/1.464913.

[23] Lee, C.; Yang, W.; Parr, R. G., Development of the Colle-Salvetti correlation-energy formula into a functional of the electron density. *Phys. Rev. B*, **1988**, *37*, 785-789, DOI: 10.1103/PhysRevB.37.785.

[24] Delley, B., From molecules to solids with the DMol3 approach. *J. Chem. Phys.*, *2000*, *113*, 7756-7764, DOI: 10.1063/1.1316015.

[25] Andzelm, J.; Kölmel, C.; Klamt, A., Incorporation of solvent effects into density functional calculations of molecular energies and geometries. *J. Chem. Phys.*, **1995**, *103*, 9312-9320, DOI: 10.1063/1.469990.